International Journal of Plant Production
https://doi.org/10.1007/s42106-019-00042-y

RESEARCH

Stochastic Estimation of Potential and Depleted Productivity of Soybean Grain and Oil

Marcelo Rodrigues Alambert[1] · Renan Caldas Umburanas[1] · Felipe Schwerz[1] · Klaus Reichardt[2] · Durval Dourado-Neto[1]

Received: 14 October 2018 / Accepted: 4 March 2019

Abstract

Soybean is one of the most important food crops around the world. Despite its economic importance, the effect of sowing date and climatic conditions on soybean development and productivity of grain and oil has not yet been studied in detail. Such a study can yield valuable information regarding the interaction of this crop with its environment. In this context, the aim of this study was to estimate the soybean potential productivity of grains and oil for eight sowing dates, using historical series of climate data from Piracicaba (SP), Brazil. For this a stochastic model is proposed, with truncated normal distribution for maximum, minimum and average temperature data. The information generated in this study is important in order to provide farmers with relevant information about the importance of an adequate sowing date, as well as to further understand of the influence of the climate variations on soybean production. The September 1 sowing date, without lack of water, provides more adequate conditions for accumulated dry matter, grain and oil productivity. It was concluded that: (i) the stochastic model (Potential and Depleted Model for Soybean Grain and Oil Production) can be used as a valuable tool for analyzing variability and complex interactions between plants and climate conditions. In this model, the air temperature and global radiation parameters were adequate to estimate the duration of the crop cycle, dry matter production, photoassimilates partition, and grain and oil productivity of soybean plants grown in different sowing dates in Piracicaba–SP; (ii) considering the historical data of air temperature, global radiation and other optimal ecophysiological needs for the crop, the model results define September as best period for sowing soybean in Piracicaba (SP), Brazil.

Keywords Climate parameters · Crop growth models · Photoassimilates partition · Sowing date

Introduction

Soybean (*Glycine max* (L.) Merril) is an important source of vegetable oil and protein cultivated in several regions of the planet. It can be used for human and animal consumption, as well as industrial application and biofuel production, mainly. In 2017, 352 million tons of soybeans were produced in the world (FAO 2019) of which 114.07 million tons were produced in Brazil (Conab 2017). However, the current rate of seed productivity increase is insufficient to meet the goal of the United Nations to double food production by 2050 (Ray et al. 2013). In order to meet future demand for grain, bran and biodiesel, it is important to find management procedures that lead to greater potential for soybean production worldwide. Brazil is one of the countries with the greatest potential to meet the worldwide increase in demand for food, and especially demand for soybeans. In this context, efforts must be made to increase soybean productivity.

Thus we propose a crop growth model to estimate the oil productivity as well as the yield of soybean grains, based on a climatic series of a given region. With the use of crop growth models within a climatic series, it is possible to estimate the performance plants in these environments, also to seek management strategies that maximize soybean grain, oil and protein productivity (Dourado Neto et al. 1998; Marin et al. 2014; Martins et al. 2017). This can optimize the use of resources,

Marcelo Rodrigues Alambert and Renan Caldas Umburanas contributed equally to this work.

✉ Renan Caldas Umburanas
renan.umburanas@gmail.com

[1] Luiz de Queiroz College of Agriculture (ESALQ), University of São Paulo (USP), Piracicaba 13418-900, Brazil

[2] Center of Nuclear Energy in Agriculture (CENA), University of São Paulo (USP), Piracicaba 13400-970, Brazil

Published online: 12 April 2019

reduce the cost and time of research, and anticipate results with high reliability. Also could reduce the probability of crop frustration. The model was tested using a representative climatic series for one soybean producing region of Brazil. This model also contributes to estimating potential productivity at different sowing times, based in air temperature, rainfall and solar radiation interception during the soybean crop cycle.

Among the available soybean sowing dates significant changes can occur in environmental conditions, affecting soybean productivity and grain composition. For example, in some regions, late sowing dates are known to lead to lower grain productivity and grain oil content (Pierozan-Junior et al. 2017; Umburanas et al. 2018). Models can help to choose the best sowing date because they can assess complex interactions between the plant and climatic conditions. In addition, the oil content will be lower when the maturation is closer to periods of lower temperatures, more precisely, with greater interaction during the grain filling phase. The delay of the sowing date can reduce productivity due to a shortening of the cycle and grain filling period (De Bruin and Pedersen 2008; Fatichin et al. 2013; Meotti et al. 2012; Umburanas et al. 2019). From early sowing to late sowing, the length of both vegetative and grain-filling phases are reduced, and consequently reducing productivity (Egli and Cornelius 2009).

Plant growth and development are a function of accumulated biomass through photosynthesis. Biomass production in plants depends upon the quantity of absorbed photosynthetically active radiation (PAR_a) by leaves and the efficiency with which the leaves can convert the solar radiation into assimilates through photosynthesis. Thus, the intercepted photosynthetically active radiation (PAR_i) that is converted into biomass reveals the radiation use efficiency (RUE) by the species (Monteith 1977; Van Heerden et al. 2010). All these concepts were considered in the proposed model.

Despite being a robust tool, plant growth models are still little used in soybean cultivation studies, mainly in Brazil. The present study aims to estimate the potential productivity of grains and oil, using climate data from Piracicaba (SP), Brazil. The proposed model considers the eco-physiological characteristics of the soybean crop in response to climate data. In a stochastic way, the model estimates leaf area index, PAR_i, cycle length, photoassimilates partition, accumulated dry matter, attainable and depleted productivity of grains and oil including consideration of its advantages and limitations.

Materials and Methods

The "Potential and Depleted Model for Soybean Grain and Oil Production" (PDMSO) is proposed and shown in Fig. 1. This model is based on the model *Light Interception and Utilization*–LINTUL (Bouman et al. 1996). For the development of PDMSO, statistical tools were incorporated into LINTUL to improve the determination of grain and oil productivity in relation to variability and climate. These tools generate random values of air temperature between the upper and lower limits of the historic minimum and maximum temperatures (°C). The process was simulated thousand times for each day of the crop growth cycle.

PDMSO has entry data as shown in the first line of Fig. 1 and the crop growth cycle is sized according to the sum of degree-days required for the closing of the crop growth cycle. Soybean development parameters are shown in Table 1. Climate elements as rainfall, irrigation, air relative humidity and actual evapotranspiration are considered as optimum, as well as the availability of nutrients, pest, disease and weed control.

Sowing Dates

Eight sowing dates were considered in the simulations, all in the first and the 15th day of the months of September, October, November and December, covering a wider period than the officially recommended sowing period for Brazil. In the Midwest region, the best season begins on October 20 and ends on December 10, and may be extended until 20 December in areas of well corrected soil, of high fertility and high-tech management (Embrapa 2005). In general, in the South, Southeast and Midwest regions of Brazil the highest grain productivities occur when soybeans are planted between the second half of October and November (Embrapa 2005, 2007).

Phenology and Growth Analysis

Carbon Partition

Available carbohydrates are allocated to the different plant organs in defined proportions according to the phenological stages (Fehr and Caviness 1977) and aiming to obtain daily partition coefficients for each organ (root, stem, leaf and reproductive organs), the PDMSO model uses an allocation function for each organ, so that the partition to all organs adds up 1.0 in all relative development stages (Ds) (Penning de Vries et al. 1989).

Soybean Relative Development

The relative development of the crop depends on the air temperature. The rate and moment of the appearance of the different organs depends on the energy availability for the system. During the period before anthesis, for a given soybean variety, the critical photoperiod (13 h) does not change for different sowing dates, but the vegetative growth period is the longer the earlier sowing is performed in relation to the critical photoperiod.

The longer the period prior to anthesis higher values of leaf area index (LAI, m^2 [leaf] m^{-2} [soil]) can be achieved,

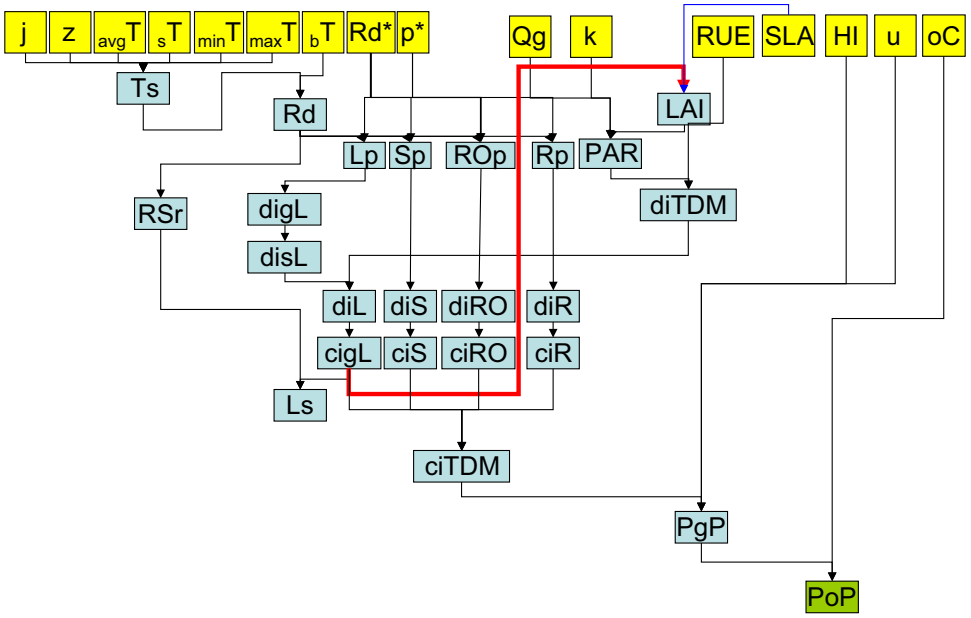

Fig. 1 Stochastic model for the estimation of the potential soybean oil productivity. (I) Entry values (first line): Julian day (j); a random variable normally distributed with zero mean and unity standard deviation, generated stochastically with uniform distribution between 0 and 1 (z); average air temperature (avgT, °C); standard deviation (sT, °C); minimum air temperature (minT, °C); maximum air temperature (maxT, °C); basal crop temperature (bT, °C); critical relative development values (Rd); carbohydrate partition (p); global radiation (Qg, MJ m^{-2} day^{-1}); radiation extinction coefficient (k); radiation use efficiency (RUE, g MJ^{-1}); specific leaf area (SLA, m^2 g^{-1}); harvest index (HI, kg kg^{-1}); grain water (u, kg kg^{-1}) and oil (β, kg kg^{-1}) contents. (II) Calculation variables: simulated average daily temperature (Ts, °C); soybean crop relative development (Rd); leaf area index (LAI, m^2 m^{-2}); carbohydrate partition to the leaf (Lp, kg kg^{-1}), stem (Sp, kg kg^{-1}), reproductive organs (ROp, kg kg^{-1}), and root (Rp, kg kg^{-1}); photosynthetic active radiation (PAR, MJ m^{-2} day^{-1}); relative senescence rate (RSr, kg kg^{-1}); daily increment of green leaf (digL, kg ha^{-1} day^{-1}), senescence leaf (disL, kg ha^{-1} day^{-1}), total leaf (diL, kg ha^{-1} day^{-1}), stem (diS, kg ha^{-1} day^{-1}), reproductive organ (diRO, kg ha^{-1} day^{-1}), dry matter of root (diR, kg ha^{-1} day^{-1}), and total dry matter (diTDM, kg ha^{-1} day^{-1}); cumulative increment of dry matter of green leaf (cigL, kg ha^{-1}), stem (ciS, kg ha^{-1}), reproductive organ (ciRO, kg ha^{-1}) and root (ciR, kg ha^{-1}); Leaf senescence (Ls, kg ha^{-1}), and total dry matter (ciTDM, kg ha^{-1}). (III) Outlet variables: potential grain productivity (PP, kg ha^{-1}) and potential oil productivity (PoP, kg ha^{-1})

Table 1 Soybean development parameters used in the PDMSO model

Parameter	Values	References
Extinction coefficient (k)	0.7	Müller et al. (2017)
Critical leaf area index (LAI)	4.0	Board and Harville (1992)
Initial leaf area index (LAI)	0.017	Santos et al. (2003)
Radiation use efficiency (RUE)	2.3 g MJ^{-1}	Sinclair et al. (1992)
Specific leaf area (sLA)	0.038 m^2 g^{-1}	Wu et al. (2017)
Lower basal temperature	10 °C	
Higher basal temperature	40 °C	
Lower optimum temperature	25 °C	Setiyono et al. (2007)
Higher optimum temperature	30 °C	Setiyono et al. (2007)
∑ degree-days for emergence (ADSe)	80 °C day	
∑ degree-days from emergence to anthesis (ADSa)	500 °C day	
∑ degree-days from anthesis to maturity (ADSm)	888 °C day	
Harvest index (HI)	0.55 kg kg^{-1}	Spaeth et al. (1984)
Depletion factor (df)	0.65 kg kg^{-1}	
Grain water content (u)	0.12 g g^{-1}	

resulting in a higher productivity potential. There is a limit to increase productivity in relation to LAI, above which there is no plant response. The interception of PAR becomes maximum at the R_1 stage when the LAI for soybeans is between 3.5 and 4.0 (Board and Harville 1992). In this study, the photoperiod will not exert effect on the results, because it will be considered above the critical photoperiod. Since the crop development rate is altered by day length, this effect is included in the PDMSO model by modifying the growth rate of the thermal unit. After anthesis, the photoperiod is not decisive for the definition of the phenological stages. The model uses the scale that is the relative crop development (Rd) for the vegetative phase, with a value of 0.0 at emergence and 1.0 at anthesis (Eq. 1), and for the reproductive phase, with a value of 2.0 at maturity (Eq. 2) (Penning de Vries et al. 1989):

$$\mathrm{Rd_v V_n} - \mathrm{V_{n-1}} = \frac{\sum_{t=t_{n-1}}^{t_n} (Ts - Tb)}{\sum_{t=t_0}^{t_v} (Ts - Tb)}, \tag{1}$$

$$\mathrm{Rd_r R_n} - \mathrm{R_{n-1}} = 1 + \frac{\sum_{t=t_{n-1}}^{t_n} (Ts - Tb)}{\sum_{t=t_0}^{t_r} (Ts - Tb)}, \tag{2}$$

where t is the time in days after sowing (DAS), t_n refers to the day of the nth evaluation, t_{n-1} to the previous evaluation, t_0 to the first evaluation, t_v to the final date of the vegetative period (for $t_0 \le t < t_v$ – VE–R_1), t_r to the final date of the reproductive period (for $t_0 \le t \le t_r$ – R_1–R_8), Rd_v to the vegetative phase, and Rd_r to the reproductive phase.

Accumulated Degree-Days

The thermal sum values are dependent on the maturation cycle, growing region and adopted value of basal temperature. This study uses the following thermal sums related to the early maturity group of soybean cultivars, the most used group by growers in Brazil: (i) between sowing and emergence, 80 °C day (ADSe); (ii) between the emergence and anthesis, 500 °C day (ADSa), and (iii) in the reproductive phase between anthesis and maturation, 888 °C day (ADSm).

Leaf Area Index

Vegetative Phase The calculation of the intercepted photosynthetically active radiation (PAR) is dependent on the LAI, because leaves are the organs of highest photosynthetic activity. In the period of emergency (Ve) until before the start of blooming (R_1). At this stage, the temperature is the predominant environmental factor, both for the final leaf size and for the rate of new leaf appearance (Hofstra 1972). In this initial period, the leaf area increases exponentially until the end of juvenile phase:

$$LAI = LAI_0 \cdot e^{cr_e \cdot T_{EF} \cdot t}, \tag{3}$$

where cr_e (°C day^{-1}) is the relative growth rate of the leaf area during its exponential growth, T_{EF} is the daily effective temperature (°C) and t (day) the time. Therefore, for daily changes (t + Δt), we have:

$$LAI_{t+\Delta t} = LAI_t \cdot e^{cr_e \cdot T_{EF} \cdot \Delta t}, \tag{4}$$

where LAI_t is the leaf area index referring for the tth day after emergence, and $LAI_{t+\Delta t}$ for the (t + Δt)th day. So, for the PDMSO model the rate of increase in leaf area is calculated during juvenile growth by:

$$\left(\frac{\Delta LAI}{\Delta t}\right)_{Ve-Vn} = \frac{LAI_{t+\Delta t} - LAI_t}{\Delta t} = \frac{LAI_t.e^{cr_e \cdot T_{EF} \cdot \Delta t} - LAI_t}{\Delta t} = \frac{LAI_t(e^{cr_e \cdot T_{EF} \cdot \Delta t} - 1)}{\Delta t}. \tag{5}$$

Reproductive Phase After the juvenile period, the increase in leaf area depends on the availability of assimilates. The growth of leaf area is calculated by the model by multiplying the increase in mass of the leaf partition (Lp) by the specific leaf area (SLA) of new leaves. Thus, SLA operates as the ratio of the leaf area and its biomass:

$$\left(\frac{\Delta LAI}{\Delta t}\right)_{(R_1-R_8)} = Lp \cdot SLA. \tag{6}$$

A relative mortality rate (RMR, day^{-1}) defines the rate of senescence of leaves, and the LAI is obtained by integrating the result of the leaf growth rate and leaf senescence rate over time.

The use of global radiation by crops depends on the leaf area capable of interception. At the beginning of soybean development, LAI is low until 20 DAS, when there is exponential growth until the crop reaches the critical LAI, which is around 3.5–4.0 (Board and Harville 1992). From there on the intercepted radiation remains at that level for the period before senescence starts and thereafter decreases with the progression of leaf loss.

Biomass Production and Radiation Use Efficiency

Under optimum development conditions, the solar radiation use efficiency (RUE, g [dry matter] MJ^{-1} [PAR]) is regarded as linear in time (Monteith 1972) and is the ratio of the rate of biomass production (g m^{-2} day^{-1}) and the rate of absorbed radiation (PAR_a, MJ m^{-2} day^{-1}). PAR_a depends on LAI, the incident daily global radiation rate (Qg, MJ m^{-2} day^{-1}), and the intercepted fraction of the PAR, corresponding to about 50% of the total daily radiation. It is assumed that the interception of the radiation increases with the increase of LAI, since the light transmittance diminishes as it enters the canopy. Thus, the specific light extinction

coefficient (k) characterizes a negative exponential function of the leaf area index.

Applying the radiation transmission law of Beer–Lambert–Bouguer, we can say that:

$$PAR_a = 0.5Q_g\left[1 - \exp^{(-k.LAI)}\right]. \tag{7}$$

We adopted a critical LAI (Table 1) beyond which absorption remains constant. The daily RUE is considered constant because most leaves are not exposed to saturating radiation intensities during most of the day (Monteith 1972; Sinclair 1991; Sinclair and Muchow 1999).

The daily increment of total dry matter (diTDM) of the crop (g [dry matter] ha^{-2} day^{-1}) can then be calculated by multiplying PAR_a by the constant RUE:

$$\text{diTDM} : \frac{\Delta W}{\Delta t} = RUE \cdot \text{PAR}_a. \tag{8}$$

Finally, the total dry matter (ciTDM) of the crop is obtained integrating Eq. (8) along time.

Photoassimilates Partition

The partition of assimilates can be estimated by the difference in dry matter of the different plant organs (leaves, roots, stems and pods) between two consecutive assessments (growth analysis), divided by the difference of the relative development (Rd) of each stage, in percentage terms. The sum of the partitions for the different plant organs, in a given time (usually using phenological scale) is in general taken equal to 1.0.

Data for the daily partition coefficient of the photoassimilates were obtained by Penning de Vries et al. (1989) and used in the PDMSO model to estimate the partition and the potential productivity of the soybean crop.

Photoassimilate Conversion

Glucose from photosynthesis is converted mainly into five basic organic constituent components of plant tissues: carbohydrates (CHO, %), proteins (PRO, %), lipids (LIP, %), lignin (LIG, %) and organic acids (ORA, %) at a cost of conversion dependent of the type of organ and plant species. The conversion cost denotes the photosynthetic efficiency of each species in the transformation of solar energy into assimilates (Penning de Vries et al. 1989).

For the calculation of the conversion efficiency (CE_i) for leaf (l), stem (s), root (r) and reproduction organs (ro), using the contents (T_i) of CHO, PRO, LIP, LIG, ORA, and minerals (MIN), and also the conversion efficiency (CE), i.e. gram of product per gram of glucose, we have:

$$\begin{aligned} \text{CE}_{(l)} = {} & \text{T}_{(l)\text{CHO}} \cdot \text{CE}_{\text{CHO}} + \text{T}_{(l)\text{PRO}} \cdot \text{CE}_{\text{PRO}} \\ & + \text{T}_{(l)\text{LIP}} \cdot \text{CE}_{\text{LIP}} + \text{T}_{(l)\text{LIG}} \cdot \text{CE}_{\text{LIG}} \\ & + \text{T}_{(l)\text{ORA}} \cdot \text{CE}_{\text{ORA}} + \text{T}_{(l)\text{MIN}} \cdot \text{CE}_{\text{MIN}}, \end{aligned} \tag{9}$$

$$\begin{aligned} \text{CE}_{(s)} = {} & \text{T}_{(s)\text{CHO}} \cdot \text{CE}_{\text{CHO}} + \text{T}_{(s)\text{PRO}} \cdot \text{CE}_{\text{PRO}} \\ & + \text{T}_{(s)\text{LIP}} \cdot \text{CE}_{\text{LIP}} + \text{T}_{(s)\text{LIG}} \cdot \text{CE}_{\text{LIG}} \\ & + \text{T}_{(s)\text{ORA}} \cdot \text{CE}_{\text{ORA}} + \text{T}_{(s)\text{MIN}} \cdot \text{CE}_{\text{MIN}}, \end{aligned} \tag{10}$$

$$\begin{aligned} \text{CE}_{(r)} = {} & \text{T}_{(r)\text{CHO}} \cdot \text{CE}_{\text{CHO}} + \text{T}_{(r)\text{PRO}} \cdot \text{CE}_{\text{PRO}} \\ & + \text{T}_{(r)\text{LIP}} \cdot \text{CE}_{\text{LIP}} + \text{T}_{(r)\text{LIG}} \cdot \text{CE}_{\text{LIG}} \\ & + \text{T}_{(r)\text{ORA}} \cdot \text{CE}_{\text{ORA}} + \text{T}_{(r)\text{MIN}} \cdot \text{CE}_{\text{MIN}}, \end{aligned} \tag{11}$$

$$\begin{aligned} \text{CE}_{(ro)} = {} & \text{T}_{(ro)\text{CHO}} \cdot \text{CE}_{\text{CHO}} + \text{T}_{(ro)\text{PRO}} \cdot \text{CE}_{\text{PRO}} \\ & + \text{T}_{(ro)\text{LIP}} \cdot \text{CE}_{\text{LIP}} + \text{T}_{(ro)\text{LIG}} \cdot \text{CE}_{\text{LIG}} \\ & + \text{T}_{(ro)\text{ORA}} \cdot \text{CE}_{\text{ORA}} + \text{T}_{(ro)\text{MIN}} \cdot \text{CE}_{\text{MIN}}. \end{aligned} \tag{12}$$

Plant Dry Matter

The cumulative increment dry matter (ci) of each organ is the result of the product of the net photosynthesis (diTDM) by the conversion efficiency (CE); and the partition of the respective carbohydrate (P). (i) as leaf partition (Lp), stem partition (Sp), root partition (Rp), reproductive organ partition (ROp):

$$\text{ci}_{(i)} = \text{diTDM}_{(i)} \cdot \text{P}_{(i)} \cdot \text{CE}_{(i)}. \tag{13}$$

Therefore, the cumulative increment of total dry matter (ciTDM, kg ha^{-1}) is:

$$\text{ciTDM} = \text{cigL} + \text{ciS} + \text{ciRO} + \text{ciR}. \tag{14}$$

Stochastic Procedure to Determine Oil Content

Distribution of Asymmetric Triangular Probability The asymmetric triangular distribution is used when it is possible to determine the most probable value of the random variable, its minimum and maximum values, and when a linear function seems appropriate for the description of the distribution of the error values of the variables. Given these requirements, the triangular distribution can be used because it is a good model between the normal distribution and the rectangular distribution.

The area under the curve of the normal distribution plus or minus the standard deviation of one mean corresponds to 0.6827. The areas under the curve of the triangular and rectangular distributions are 0.64983 and 0.57735 respectively (Bressan 2002). This probability distribution is used in two situations: (i) when the objective is to obtain an approximation in the absence of data, which allows adjusting a more adequate distribution, or (ii) when only the most probable (m), minimum (a) and maximum (b) values of the variable are known, but not much is known about the empirical distribution of the data (Bressan 2002).

When the values of magnitude in the variable under study have a central tendency, being more likely with values close to the mean value, we use the normal distribution, or the triangular distribution, the latter with a probability density function of the random variable triangular (Bressan 2002):

$$f(x) = \begin{cases} \frac{2\,(X-a)}{(m-a)(b-a)} & if \quad a \le X \le m \\ \frac{2(b-X)}{(b-m)(b-a)} & if \quad m < X \le b \\ 0 & if\ X\ <\ a \text{ ou } X\ >\ b \end{cases} \tag{15}$$

The distribution function of the triangular random variable is given by:

$$f(x) = if \begin{array}{cc} X < a & 0 \\ a \le X \le m & \frac{(X-a)^2}{(m-a)\,(b-a)} \\ m < X \le b & 1 - \frac{(b-X)^2}{(b-m)\,(b-a)} \\ b \le X & 1 \end{array} \tag{16}$$

The mean and variance are determined according to the following equations:

$$E\,(X) = \frac{(a+m+b)}{3}, \tag{17}$$

$$Var(X) = \frac{\left(a^2+m^2+b^2-m\,a-a\,b-m\,b\right)}{18}. \tag{18}$$

Normal Symmetric Truncated Probability Distribution It is used to fit mixed linear models in which the distributions of the random effects are asymmetric normal multivariate and that can have normal distribution if the asymmetry parameter is equal to zero.

The symmetric truncated normal probability distribution (a, b, μ, σ^2) is given by the following expression (Eaton and Kortum 2002):

$$f(x) = \begin{array}{c} 0 \\ \frac{\frac{1}{\sqrt{2\pi\sigma^2}}\exp\left\{-\frac{1}{2}\left(\frac{x-\mu}{\sigma}\right)^2\right\}}{\{P(x<a)+P(x>b)\}} \\ 0 \end{array} \quad \begin{array}{c} x \le a \\ if\ \ a < x < b, \mu \in R, \sigma^2 > 0 \\ x \ge b \end{array} \tag{19}$$

on what *f* refers to the density function of the standard normal; F to its cumulative distribution; and σ^2 to the corresponding non-truncated normal variance.

The mean (μ_{TS}) and variance (σ^2_{TS}) of the symmetric truncated normal probability distribution are thus calculated:

$$\mu_{NTS} = \frac{(a+b)}{2}, \tag{20}$$

$$\sigma^2_{NTS} = \sigma^2\left\{1 - \left[\frac{b\cdot f(b) - a\cdot f(a)}{F(b)-F(a)}\right] - \left[\frac{f(b)-f(a)}{F(b)-F(a)}\right]\right\}. \tag{21}$$

Potential grain and oil productivity

The potential grain productivity (PgP, kg ha^{-1}) of the soybean is given by:

$$\mathrm{PgP} = \mathrm{HI}\cdot \mathrm{TDM}/(1-\mathrm{u}), \tag{22}$$

where *HI* is the harvest index and *u* the grain water content, based on mass (Table 1). The potential oil productivity (PoP, kg ha^{-1}) represents between 18 and 22% of PgP. For the determination of the oil content (Oc), the stochastic procedure was used. The values varied around the average of 19%, with extremes of 18.05 and 20.9%. The potential oil productivity is given by:

$$\mathrm{PoP} = \mathrm{PgP}\cdot \mathrm{Oc}. \tag{23}$$

Depletion Factor

The depletion factor estimates the reduction of the potential productivity taking into account the reality of the field conditions. In general, growing areas are extensive and is not always possible at the best time or place in the sown area the detailed control of nutritional deficiencies, diseases, pests and weeds, and water stress. Thus, the depletion factor reduces the potential productivity to the actual productivity. This study adopted a reduction of 35% of the potential productivity (Sinclair et al. 1992).

Climate Variables

The potential productivity of soybean oil was estimated for Piracicaba (SP), Brazil (22°42′S, 47°38′W, altitude of 546 m above sea level), based on historical series of climate variables temperature (maximum, minimum and average) from 1966 to 2009 (40 years) and global radiation from 1978 to 2009.

Temporal Variation of Air Temperature in Piracicaba (SP)

Air temperature along with solar radiation are the most important production factors for the definition of crop potential productivity. Soil water and other climatic components define productivity depletion.

The stochastic simulation of air temperature with 1000 samples were applied to historical data of daily average minimum, average, and maximum temperatures (Fig. 2). The average daily temperature equals the average annual temperature (21.8 °C) in late April and early October.

The average daily temperatures throughout the year (Fig. 2) are within the recommended values as upper and lower basal temperatures for soybean, respectively 10 and 40 °C.

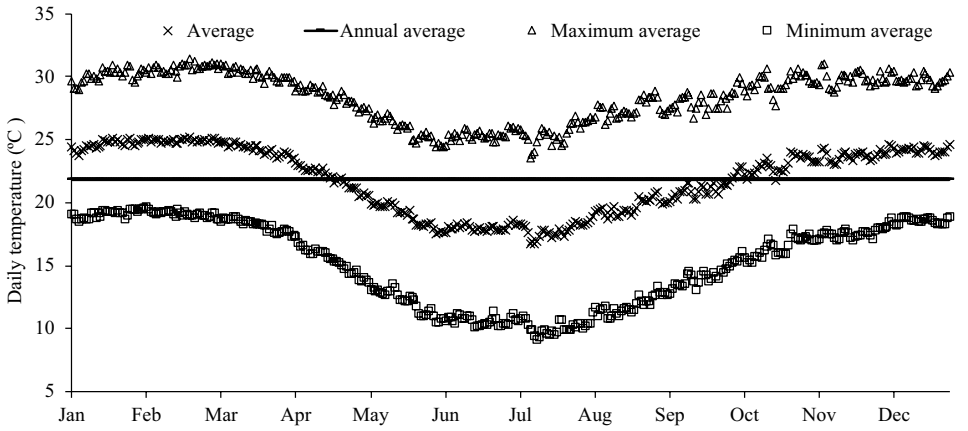

Fig. 2 Stochastic simulation of air temperature with 1000 samples applied to historical data of average daily temperature (mT, °C), average daily maximum (T_M, °C) and average daily minimum (Tm, °C) and the annual average temperature for 43 years (1966–2009) in Piracicaba (SP), Brazil

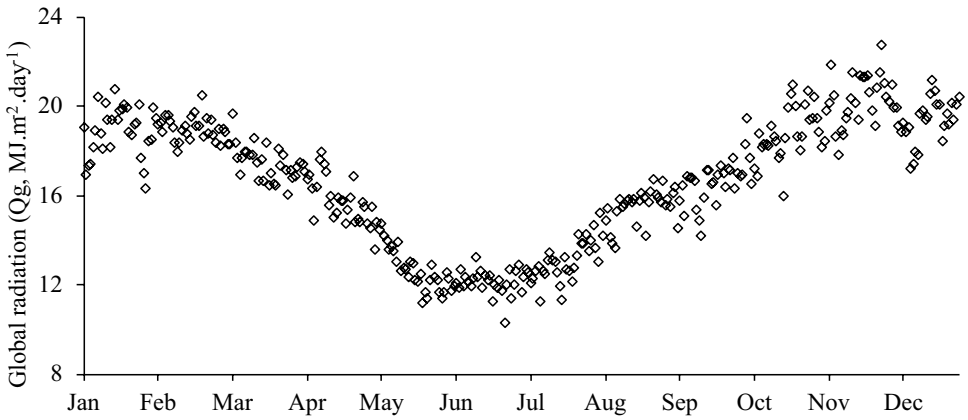

Fig. 3 Stochastic simulation with 1000 samples applied to historical data of average daily global radiation (MJ m^{-2} day^{-1}) for 43 years (1966–2009) in Piracicaba–SP, Brazil

Despite the fact that the months of September and October present minimum temperatures below the basal minimum temperature of 10 °C, the average daily temperature is always above this level. The basal upper temperature is rarely reached by the daily maximum temperature.

Temporal Variation of Radiation in Piracicaba (SP)

Historical data of average daily radiation (MJ m^{-2} day^{-1}) covering the period from 1966 to 2009 in Piracicaba are shown in Fig. 3.

Global Radiation and Intercepted Photosynthetic Active Radiation

The photosynthetically active radiation (PAR, 400–700 nm) is approximately 50% of global solar radiation and varies with radiation intensity (Monteith 1972). The PAR intercepted by the crop canopy is a function of the LAI, the incident global radiation, and light extinction coefficient.

Statistical Analysis

Given the natural variability of climate data, the use of a probabilistic tool was necessary to quantify the uncertainties in the stochastic model of maximum temperature parameters, minimum temperature and potential productivity average. In the stochastic procedure a variable is generated following a uniform distribution between 0 and 1. Subsequently, this value is turned into a random variable (z) following the normal distribution, zero mean and unit standard deviation {z (0, 1)}, according to routine computation (in Visual Basic) (Maia and Dourado Neto 2004). A stochastic simulation was inserted into the model, with 1000 samples for the determination of the productivities, using the truncated normal probability distribution for daily temperature values. To determine the oil content a stochastic procedure was also used, including a computational routine (in Visual Basic), according to Maia and Dourado Neto (2004).

Results

Climate Conditions

As sowing date is delayed, the maximum PAR incident (November and December) is obtained in the beginning of the soybean crop cycle. In the first sowing date (September 1), the culture reaches the maximum PAR around 40 after sowing (DAS), while the last sowing date (December 15), the maximum PAR is until 45 DAS, then decreases.

The interception of the radiation decreases with the increase of leaf senescence. In the first sowing date this decline starts after 80 DAS, while in last sowing date at 60 DAS.

Cycle Duration

The duration of the cycle in this study, called production cycle, was divided into vegetative phase (V), which extends from emergence (V_E) to anthesis (R_1), and the reproductive phase (R), which goes from anthesis (R_1) to full senescence (R_8). For the cycle length, periods from sowing to emergence (V_E) and from full senescence (R_8) to harvest, are not considered. Throughout the eight sowing dates, the number of days to complete the crop cycle decreased with delayed sowing due to temperature rise in the course of time.

For the September 1 sowing date there was a probability of 90.4% for a cycle length of 109 days or less to occur. For the September 15 sowing date, 93% for 106 days or less. For October 15, 97.5% for 101 days or less. For the November 15, 99.1% 98 days or less, and finally for December 15, 95% for 96 days or less.

Carbon Partition

The evaluation of the different sowing dates showed a reduction in the growth cycle, promoted by the increase of the average daily air temperature, which modified the photoassimilate partition (Figs. 4 and 5).

For the early sowing dates, the partition for leaves, roots and stems reaches periods longer than 60 DAS and the partition for storage organs starts at 50 DAS. For the last sowing dates, the partition for leaves, roots and stem

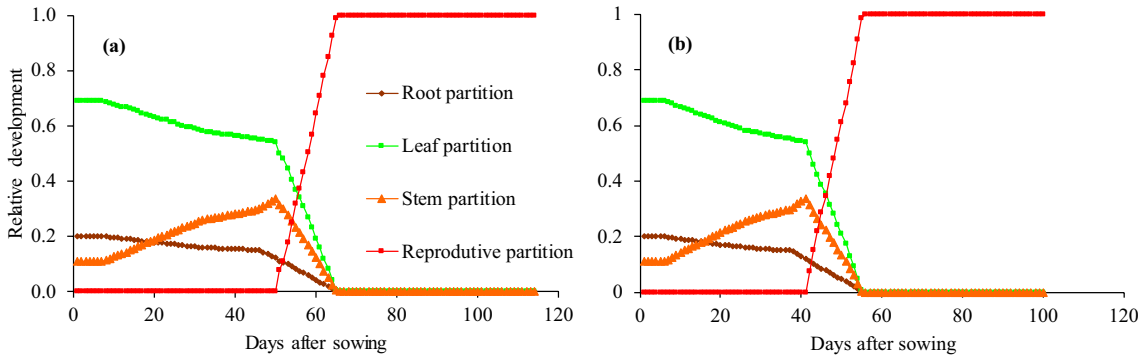

Fig. 4 Photoassimilates partition resulting from model PDMSO for the September 1 (**a**) and December 15 (**b**) sowing dates in Piracicaba (SP), Brazil (22°42′S, 47°38′W and altitude of 546 m)

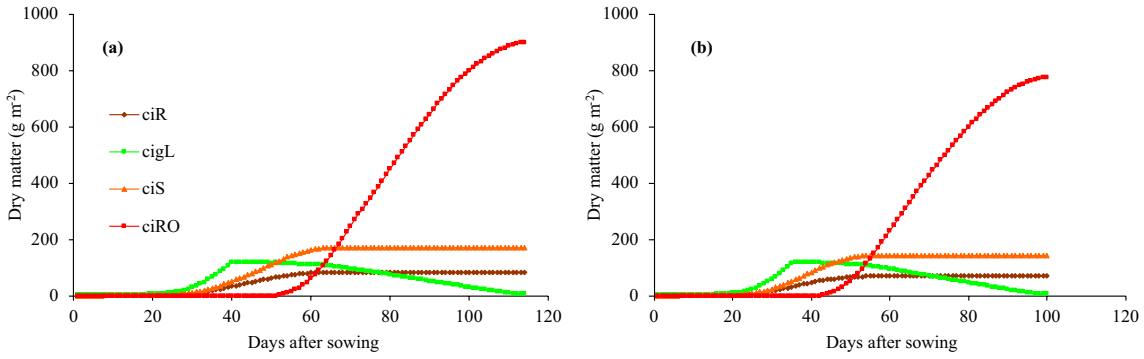

Fig. 5 Soybean dry matter estimated from PDMSO model for sowings made in September 1 (**a**) and December 15 (**b**) in Piracicaba (SP), Brazil (22°42′S, 47°38′W and altitude of 546 m). *ciR* cumulative increment in roots, *cigL* cumulative increment in green leaves, *ciS* cumulative increment in stem, *ciRO* cumulative increment in reproductive organs

occurs approximately at 56 DAS and the partition for storage organs starts at 40 DAS. Since the time evolution of the different sowing dates present very similar behavior, Fig. 4 shows only the graphs of the extreme dates, September 1 and December 15. In all graphs it can clearly be seen that when the productive organs start to be produced, the partition to leaves, stems and roots start to decline, reducing to minimum values about 10 days later.

Dry Matter Accumulation

The dry matter accumulation per organ follows a similar behavior in relation to the photo-assimilate partition (Fig. 5), as expected. The reduction of the cycle length due to the increase in air temperature, accelerates the accumulation of dry matter. We also show only the graphs of the first and last sowing dates due to the similarity of all of them. During the vegetative growth period, the dry matter accumulation of root and stem reach a peak and become stabilized at the end of the cycle at the R_8 growth stage. The growth of leaves reaches the maximum before flowering and declines to zero due to leaf senescence, also at the end of cycle (R_8). The dry matter accumulation of the reproductive organs begins at anthesis (R_1) and reaches a maximum at the end of the cycle (R_8).

As mentioned before, with the delay in sowing date the average air temperature increased during the vegetative phase, which anticipated the peak of dry matter accumulation and reduced its amount. For plants sown at the first sowing date (September 1), the dry matter of root and stem became maximum at 66 DAS and for plants sown at the last sowing date (December 15) it occurred at 56 DAS. The dry matter of green leaves became maximum at 41 DAS for plants of the first sowing date and 36 DAS for the last.

The dry matter accumulation of the reproductive organs begun at 52 DAS and ended at 114 DAS for plants sown at the first sowing date (September 1) and begun accumulation at 43 DAS and ended at 100 DAS for plants sown at the last sowing date (December 15). The maximum dry matter accumulation of the reproductive organs, which was achieved at the $R_{5.5}$ growth stage with a value nearly of 900 g m^{-2} for plants from the first and second sowing dates,

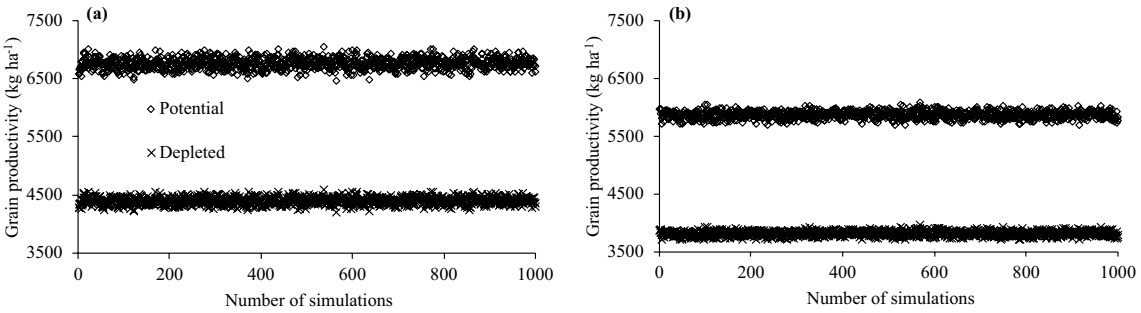

Fig. 6 Distribution of potential and depleted productivities resulting from PDMSO model for sowings made in September 1 (**a**) and December 15 (**b**), after a thousand simulations for Piracicaba (SP), Brazil (22°42′S, 47°38′W and altitude of 546 m)

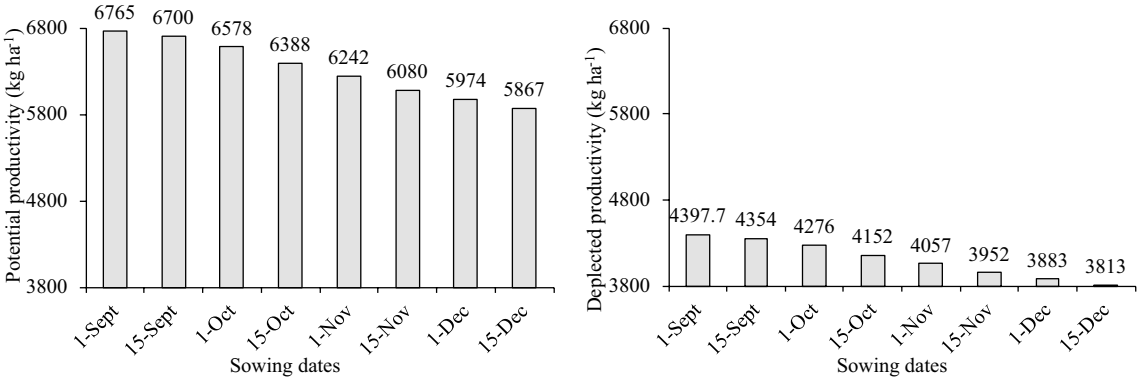

Fig. 7 Averages of potential and depleted grain productivity resulting from the PDMSO model for Piracicaba (SP), Brazil (22°42′S, 47°38′W and altitude of 546 m)

and decreased below 800 g m^{-2} for plants from the last sowing date.

Potential and Depleted Grain Productivity

Additionally, to the reduction of the crop cycle, the potential and depleted productivities were also reduced with the delay of the sowing date (Fig. 6). The best potential and depleted productivity results occur for the first sowing date and a linear decay was observed until the last sowing date (Fig. 7).

In first and second sowings dates (September 1 and 15), the distribution of the potential grain productivity (PgP) observed after a thousand sample randomization resulted in values ranging from 6500 to 7000 kg ha^{-1}, with averages of 6765 and 6700 kg ha^{-1}, respectively. For the two latest sowing dates, December 1 and 15, the amplitude of PgP was reduced to 5700–6000 kg ha^{-1}, with averages of 5974 and 5866 kg ha^{-1}, respectively, representing a decline ranging from 11.7 to 12.4% compared to the first two sowing dates, which represents the same trend for depleted productivity.

As already mentioned, for the simulations of our model a maximum RUE value of 2.3 g MJ^{-1} was adopted (Sinclair et al. 1992). Figure 8 shows the sensitivity of the model for this parameter showing how the productivity performance is altered using other RUE values reported in the literature.

With the combined use of the value of RUE and of the depletion factor, it is possible to approximate the simulation to field results. High productivities obtained at field levels range from 3300 to 3600 kg ha^{-1}. The change of the RUE to 1.72 g MJ^{-1} (Leadley et al. 1990; Muchow et al. 1993) would bring results closer to field levels without the need to apply a depletion factor.

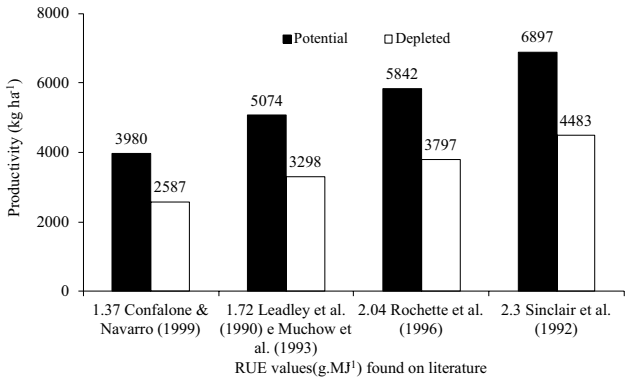

Fig. 8 Soybean potential and depleted productivity with 90% of probability corresponding to the September sowing estimated by the PDMSO model with different values of RUE (g MJ^{-1}) considering the climatic data of Piracicaba (SP), Brazil (22°42′S, 47°38′W and altitude of 546 m)

Figure 9a shows a good relation between the depleted productivity and cycle duration. The effect of the average air temperature can also clearly be seen in Fig. 9b. The amount of the average global solar radiation occurring throughout duration of the cycle (Fig. 9c) shows no correlation with the depleted productivity. The depleted oil productivity (Fig. 9d), however, followed the grain productivity, as expected.

Oil Productivity and Content

The oil productivity after randomization and simulated by the PDMSO model shows decreasing values with the delay of the sowing date (Fig. 10). From the first to the last simulated sowing date, average oil productivity decreased in average from 743 to 644 kg ha^{-1}, a reduction of 99 kg ha^{-1} or 13.3%.

The grain oil content was randomized with lower and upper limits of 18.1 and 20.9% (Penning De Vries et al. 1989). The model generated frequencies near 70% in the range from 19.0 to 19.5% oil content (Fig. 10, Table 2).

Discussion

The effects of changes in sowing date and climate conditions on the ecophysiological characteristics such as cycle duration, photoassimilate partition, dry matter production, leaf area index, photosynthetically active radiation interception, attainable and depleted productivity of grains and oil of soybean plants were assessed in this study using a stochastic model.

Sowing Date Determines the Cycle Duration of Soybean

The chosen eight sowing dates start in September 1. Officially, soybean sowings are recommended from mid-September until mid-December. The sowing should not be delayed to dates after December 15. During these three periods, the average air temperature is in an increasing trend for the Piracicaba region (Fig. 2), which accelerates plant growth (Setiyono et al. 2007). Therefore, the duration of the crop cycles simulated by the PDMSO showed a decrease in the course of time. For the September 1 sowing date the thousand simulations indicate a probability of 90.4% for a cycle length of 109 days or less. For the September 15 sowing date, 93% for 106 days or less, this being the sowing date of largest cycle. The shortest cycle was for the last sowing

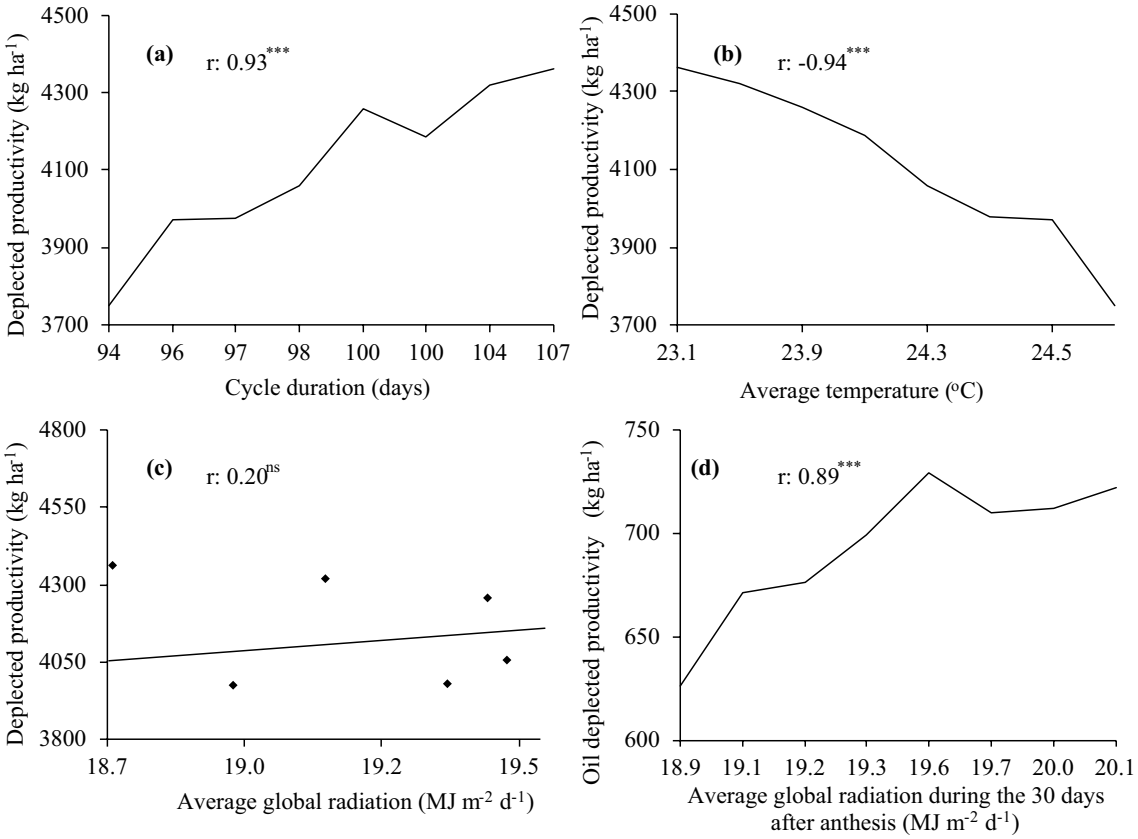

Fig. 9 Depleted grain productivity resulting from the PDMSO model correlated to **a** cycle duration; **b** average temperature during the cycle; **c** average global radiation over the cycle and; **d** average global radiation during the 30 days after anthesis using climatic data of Piracicaba (SP), Brazil (22°42′S, 47°38′W and altitude of 546 m)

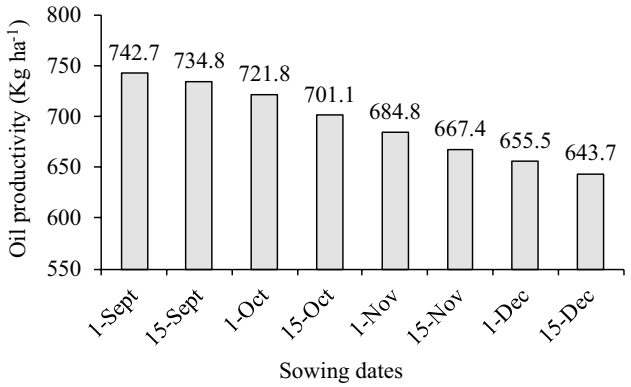

Fig. 10 Average potential oil productivity at different sowing dates estimated by the Potential and Depleted Model for Soybean Grain and Oil Production (PDMSO), for Piracicaba (SP), Brazil (22°42′S, 47°38′W and altitude of 546 m)

date, December 15, with a 95% probability for 96 days or less. This shows a total difference of 10 days, which might be of significance for soybean growers in this area.

Table 2 Frequency of oil content results at different sowing dates from the Potential and Depleted Model for Soybean Grain and Oil Production (PDMSO) after a thousand simulations, for Piracicaba (SP), Brazil (22°42′S, 47°38′W, altitude 546 m)

	Oil content (%)			
	18.0–18.5	18.5–19.0	19–19.5	19.5–20.0
1-Sep	16	117	757	110
15-Sep	12	138	745	105
1-Oct	15	199	687	99
15-Oct	4	206	693	97
1-Nov	12	212	673	103
15-Nov	8	207	678	107
1-Dec	11	218	656	115
15-Dec	12	197	689	102

Air Temperature Affects the Carbon Partition of Soybean

The different sowing dates simulated by PDMSO modified the photoassimilate partition, mainly due to the increase in

the average air temperature. For the September 1 sowing date, the partition of carbon to storage organs started at 50 DAS, while for the December 15 date the partition started at 42 DAS, 8 days before. For all sowing dates it was observed that when the reproductive organs start to be produced, the carbon partition to leaves, stems and roots start to decline, reducing to minimum values close to zero, about 10 days later.

Regarding the partition of assimilates produced, the biomass accumulated in the leaves decreased gradually throughout the crop cycle, especially during the maturation stage due to the senescence of the lower leaves and the reallocation of the assimilates for grain filling (Fig. 5). The results observed are consistent with those of Taiz et al. (2017) who reported that the priority order of the assimilated partition is determined according to the stage of crop development: roots, leaves and vegetative buds are the priority in the vegetative stage, and flowers, pods and grains, in the reproductive stage.

The translocation of assimilates to sink organs is determined by factors such as the proximity of source to sink; thus, the leaves allocated in the lower layer direct their assimilates to the roots, while the leaves of the upper layer send assimilates to the growing apices, and the leaves of the middle layer to both directions (Taiz et al. 2017).

Relationship Between Dry Matter Produced and Climate Conditions

Simulations also show that the dry matter accumulation per organ are in accordance to the photoassimilate partition, as expected. The pattern of the cumulative curves is very similar for all dates, only with anticipations up to 10 days due to cycle shortening. Between 40 and 60 DAS root, leaf, and stem accumulation of dry matter starts declining while that of the reproductive organs speeds up to about five times higher values. The results show clearly that there is an anticipation of the accumulation curves that, however did not affect the carbon accumulation in reproductive organs.

The soybean dry matter accumulation analysis, which is the response of the plant in function to the biomass produced and assimilated, may be of great importance for a better understanding of the mechanisms that influence productive efficiency of the crop in response to meteorological conditions and sowing date.

The relationship between total dry matter produced and grain and oil productivity is due to the sowing date and its interaction with climate conditions. Considering the importance of solar radiation in the process of photosynthesis, a greater use efficiency of solar radiation does not necessarily result in a higher grain and oil productivity. In this way, the same cultivar can present a lower dry matter accumulation in a given crop year, regardless of greater or lesser availabilities of solar radiation and variations in air temperature, give that this response does not be necessarily related to an increase in crop productivity (Koester et al. 2014; Petter et al. 2016).

Potential and Depleted Grain Productivity

The thousand simulations shown in Fig. 6 indicated the stability of the PDMSO program in estimating potential and depleted grain productivities. Results also show the importance of the difference between potential and depleted values, which was 35% reduction for all sowing dates. This fact evidences that there is room for grain productivity implementation through management practices. As shown in Fig. 7, the best potential and depleted productivity results occur for the first sowing date and a linear delay was observed until the last sowing date (Fig. 7). A linear regression of these results shows an average decline of 5.5 and 8.5 kg ha^{-1} of grains per day of delay of the sowing date for depleted and potential productivity, respectively.

Since the highest productivities occurred for the first sowing date, which is extremely dependent on the start of the rainy season in Piracicaba, an analysis of the cost/benefit ratio for the adoption of irrigation has to be investigated.

Oil Productivity and Content Decrease with the Delay in the Sowing Date

Simulated values of oil productivity after randomization followed the dry matter trend, as expected (Fig. 10). A linear regression of these results shows an average decline of 0.93 kg ha^{-1} of oil per day of delay of sowing date for depleted productivity. Grain oil content simulated by PDMSO show that the most frequent values fall between 19 and 19.5%, independently of the sowing date.

The decrease in the oil productivity and content with the delay of the sowing date can be related with the reduction of the cycle duration and the reduction of air temperature and solar radiation availability for the soybean plants (Figs. 2, 3). The results found in this study were confirmed by Zuil et al. (2012), Oliva et al. (2006), and Izquierdo et al. (2009), when analyzing the soybean oil content and composition for different genotypes, which observed greater effect of the air temperature and solar radiation interception in the oil content and composition.

The information generated in this study is important in order to provide farmers with relevant information about the importance of adequate sowing date, as well as to further the understanding the climate variations and soybean production. The September 1 sowing date, without lack of water, provides more adequate conditions for accumulated

dry matter, grain and oil productivity; thus, the appropriate implementation of the sowing date, can maximize the productivity of a soybean crop.

Conclusions

We proposed a model for the stochastic estimation of potential and depleted productivity of soybean grain and oil in which air temperature was the determining climatic parameter in simulation of the duration of the crop cycle, which decreased as average temperature increased.

In this model, the global radiation, when considering its average over the cycle, did not correlate with the grain and oil productivity. However, the model considers the global radiation incident 30 days after blooming as positively correlated with productivity, which is consistent because more intercepted PAR values increase accumulation of assimilates in the partition into storage organs, which resulted in higher grain and oil productivity.

Considering the historical data of air temperature, global radiation and other ecophysiological needs optimal for the crop, the model results define September as best period for sowing soybean in Piracicaba, Sao Paulo, Brazil. The model can be tested to identify the most promising sowing dates for other regions.

Stochastic statistical treatments of the truncated normal distribution for the data of temperature, and an asymmetric triangular distribution is a new approach that improved the estimation of grain and oil yields of soybean crops. For future improvements in the model, a coefficient can be inserted considering the composition of oil that may suffer small variation according to the cultivar if more accurate estimates are needed.

The PDMSO model can be used as an estimator of the potential soybean grain and oil productivity in any part of the globe. This model, including pertinent equations, also allows to simulate productivity under stress by water deficit, loss of leaf area per incidence of diseases and pests and weed competition. The proposed model was not calibrated, which could better be made with photoassimilates partition and radiation use efficiency data obtained through field measurements.

Acknowledgements We acknowledge funding from the São Paulo Research Foundation (FAPESP)—Grant no. 2016/06310-0 and 2017/24059-5 and thank financial support from Coordination for the Improvement of Higher Education Personnel (CAPES) and from National Counsel of Technological and Scientific Development (CNPq)—Grant no. 140209/2015-8).

Compliance with Ethical Standards

Conflict of interest The authors declare that they have no conflict of interest.

References

Board, J. E., & Harville, B. G. (1992). Explanation for greater light interception in narrow-vs. Wide-row. *Crop Science*. https://doi.org/10.2135/cropsci1992.0011183X003200010041x.

Bouman, B. A. M., Van Keulen, H., Van Laar, H. H., & Rabbinge, R. (1996). The 'School of de Wit' crop growth simulation models: a pedigree and historical overview. *Agricultural Systems*. https://doi.org/10.1016/0308-521X(96)00011-X.

Bressan, G. (2002). *Modelagem e simulação de sistemas computacionais* (p. 12). São Paulo: LarcPCS/EPUSP, IME/USP.

CONAB. Companhia Nacional de Abastecimento. (2017). Acompanhamento da safra brasileira de grãos. 2016/2017. http://www.conab.gov.br/OlalaCMS/uploads/arquivos/16_12_22_12_08_27_boletim_graos_dezembro_2016.pdf. Accessed 15 Jan 2018.

Confalone, A., & Navarro, M. D. (1999). Influência do "déficit" hídrico sobre a eficiência da radiação solar em soja. *Revista Brasileira de Agrociência*. https://doi.org/10.1016/0308-521X(96)00011-X.

De Bruin, J. L., & Pedersen, P. (2008). Soybean seed yield response to planting date and seeding rate in the upper Midwest. *Agronomy Journal*. https://doi.org/10.2134/agronj2007.0115.

Dourado Neto, D., Teruel, D. A., Reichardt, K., Nielsen, D. R., Frizzone, J. A., & Bacchi, O. O. S. (1998). Principles of crop modeling and simulation: I. Uses of mathematical models in agricultural science. *Scientia Agricola*. https://doi.org/10.1590/S0103-90161998000500008.

Eaton, J. & Kortum, S. (2002) Technology, Geography, and Trade. *Econometrica*. https://doi.org/10.1111/1468-0262.00352.

Egli, D. B., & Cornelius, P. L. (2009). A regional analysis of the response of soybean yield to planting date. *Agronomy Journal*. https://doi.org/10.2134/agronj2008.0148.

Embrapa. Empresa Brasileira de Pesquisa Agropecuária. (2007). Instalação da lavoura de soja: época, cultivares, espaçamento e população de plantas. CNPSO–Centro Nacional de Pesquisa de Soja. http://www.cnpso.embrapa.br/download/cirtec/circtec51.pdf. Accessed 30 Jan 2018.

Embrapa. (2005). Empresa Brasileira de Pesquisa Agropecuária. Tecnologias de Produção de Soja—Região Central do Brasil—2006 (p. 220). (Sistemas de Produção/Embrapa Soja, 9).

FAO. (2019). Crops and livestock products. http://www.fao.org/faostat/en/#data/TP . Accessed 5 Feb 2019.

Fatichin, S., Zheng, H., Narasaki, K., & Arima, S. (2013). Genotypic adaptation of soybean to late sowing in Southwestern Japan. *Plant Production Science*. https://doi.org/10.1626/pps.16.123.

Fehr, W. R., & Caviness, C. E. (1977). *Stages of soybean development* (p. 81p). Iowa: Agricultural Experimental Station.

Hofstra, G. (1972). Response of soybeans to temperature under high light intensities. *Canadian Journal of Plant Science*. https://doi.org/10.4141/cjps72-084.

Izquierdo, N. G., Aguirrezábal, L. A. N., Andrade, F. H., Geroudet, C., Valentinuz, O., & Pereyra Iraola, M. (2009). Intercepted solar radiation affects oil fatty acid composition in crop species. *Field Crops Research*. https://doi.org/10.1016/j.fcr.2009.07.007.

Koester, R. P., Skonecza, J. A., Cary, T. R., Diers, B. W., & Ainsworth, E. A. (2014). Historical gains in soybean (*Glycine max* Merr.) seed yield are driven by linear increases in light interception, energy conversion, and partitioning efficiencies. *Journal of Experimental Botany*. https://doi.org/10.1093/jxb/eru187.

Leadley, P. W., Reynolds, J. F., Flagler, R., & Heagle, A. S. (1990). Radiation utilization efficiency and the growth of soybeans exposed to ozone: A comparative analysis. *Agricultural and Forest Meteorology*. https://doi.org/10.1016/0168-1923(90)90114-L.

Maia, A. D. H. N., & Dourado Neto, D. (2004). Probabilistic tools for assessment of pest resistance risk associated to insecticidal transgenic crops. *Scientia Agricola*. https://doi.org/10.1590/S0103-90162004000500003.

Marin, F. R., Ribeiro, R. V., & Marchiori, P. E. (2014). How can crop modeling and plant physiology help to understand the plant responses to climate change? A case study with sugarcane. *Theoretical and Experimental Plant Physiology*. https://doi.org/10.1007/s40626-014-0006-2.

Martins, K. V., Dourado-Neto, D., Reichardt, K., de Jong van Lier, Q., Favarin, J. L., Sartori, F. F., et al. (2017). Preliminary studies to characterize the temporal variation of micronutrient composition of the above ground organs of maize and correlated uptake rates. *Frontiers in Plant Science*. https://doi.org/10.3389/fpls.2017.01482.

Meotti, G. V., Benin, G., Silva, R. R., Beche, E., & Munaro, L. B. (2012). Sowing dates and agronomic performance of soybean cultivars. *Pesquisa Agropecuaria Brasileira*. https://doi.org/10.1590/S0100-204X2012000100003.

Monteith, J. L. (1972). Solar radiation and productivity in tropical ecosystems. *Journal of Applied Ecology*. https://doi.org/10.2307/2401901.

Monteith, J. L. (1977). Climate and the efficiency of crop production in Britain. *Philosophical Transactions of the Royal Society B: Biological Sciences*, *181*, 277–294. https://doi.org/10.1098/rstb.1977.0140.

Muchow, R. C., Robertson, M. J., & Pengelly, B. C. (1993). Radiation use efficiency of soybean, mungbean and cowpea under different environmental conditions. *Field Crops Research*. https://doi.org/10.1016/0378-4290(93)90017-H.

Müller, M., Rakocevic, M., Caverzan, A., & Chavarria, G. (2017). Grain yield differences of soybean cultivars due to solar radiation interception. *American Journal of Plant Sciences*. https://doi.org/10.4236/ajps.2017.811189.

Oliva, M. L., Shannon, J. G., Sleper, D. A., Ellersieck, M. R., Cardinal, A. J., Paris, R. L., et al. (2006). Stability of fatty acid profile in soybean genotypes with modified seed oil composition. *Crop Science*. https://doi.org/10.2135/cropsci2005.12.0474.

Penning De Vries, F. W. T., Jansen, D. M., Ten Berge, H. F. M., & Bakema, A. (1989). *Simulation of ecophysiological processes of growth in several annual crops* (p. 271). Wageningen: Centre for Agricultural Publishing and Documentation (Pudoc).

Petter, F. A., Da Silva, J. A., Zuffo, A. M., Andrade, F. R., Pacheco, L. P., & De Almeida, F. A. (2016). Does high seeding density increase soybean productivity? Photosynthetically active radiation responses (abstract in English, text in Portuguese). *Bragantia*. https://doi.org/10.1590/1678-4499.447.

Pierozan-Junior, C., Kawakami, J., Schwarz, K., Umburanas, R. C., Del Conte, M. V., & Müller, M. M. L. (2017). Sowing dates and soybean cultivars influence seed yield, oil and protein contents in subtropical environment. *Journal of Agricultural Science*. https://doi.org/10.5539/jas.v9n6p188.

Ray, D. K., Mueller, N. D., West, P. C., & Foley, J. A. (2013). Yield trends are insufficient to double global crop production by 2050. *PLoS One*. https://doi.org/10.1371/journal.pone.0066428.

Rochette, P., Desjardins, R. L., Pattey, E., & Lessard, R. (1996). Instantaneous measurement of radiation and water use efficiencies of a maize crop. *Agronomy Journal*. https://doi.org/10.2134/agronj1996.00021962008800040022x.

Santos, J. B., Procópio, S. O., Silva, A. A., & Costa, L. C. (2003) Capture and utilization of solar radiation by the soybean and common bean crops and by weeds. *Bragantia*. https://doi.org/10.1590/S0006-87052003000100018.

Setiyono, T. D., Weiss, A., Specht, J., Bastidas, A. M., Cassman, K. G., & Dobermann, A. (2007). Understanding and modeling the effect of temperature and daylength on soybean phenology under high-yield conditions. *Field Crops Research*. https://doi.org/10.1016/j.fcr.2006.07.011.

Sinclair, T. R. (1991). Predicting carbon assimilation and crop radiation-use efficiency dependence on leaf nitrogen content. In K. J. Boote & R. S. Loomis (Eds.), *Modeling crop photosynthesis—From biochemistry to canopy* (pp. 75–94). Madison: American Society of Agronomy; Crop Science Society of America.

Sinclair, T. R., & Muchow, R. C. (1999). Radiation use efficiency. *Advances in Agronomy*. https://doi.org/10.1016/S0065-2113(08)60914-1.

Sinclair, T. R., Shiraiwa, T., & Hammer, G. L. (1992). Variation in crop radiation-use efficiency with increased diffuse radiation. *Crop Science, 32,* 1281–1284. https://doi.org/10.2135/cropsci1992.0011183X003200050043x.

Spaeth, S. C., Randall, H. C., Sinclair, T. R., & Vendeland, J. S. (1984). Stability of soybean harvest index 1. *Agronomy Journal*. https://doi.org/10.2134/agronj1984.00021962007600030028x.

Taiz, L., Zeiger, E., Møller, I. M., & Murphy, A. (2017). *Plant physiology (Portuguese version)* (6th ed., p. 888). Porto Alegre: Artmed.

Umburanas, R. C., Yokoyama, A. H., Balena, L., Lenhani, G. C., Moraes, Teixeira A., Krüger, R. L., et al. (2018). Sowing dates and seeding rates affect soybean grain composition. *International Journal of Plant Production*. https://doi.org/10.1007/s42106-018-0018-y.

Umburanas, R. C., Yokoyama, A. H., Balena, L., Dourado-Neto, D., Teixeira, W. F., Zito, R. K., et al. (2019). Soybean yield in diferent sowing dates and seeding rates in a subtropical environment. *International Journal of Plant Production*. https://doi.org/10.1007/s42106-019-00040-0.

Van Heerden, P. D. R., Donaldson, R. A., Watt, D. A., & Singels, A. (2010). Biomass accumulation in sugarcane: Unraveling the factors underpinning reduced growth phenomena. *Journal of Experimental Botany*. https://doi.org/10.1093/jxb/erq144.

Wu, Y. S., Yang, F., Gong, W. Z., Shoaib, A., Fan, Y. F., & Wu, X. L. (2017). Shade adaptive response and yield analysis of different soybean genotypes in relay intercropping systems. *Journal of Integrative Agriculture*. https://doi.org/10.1016/S2095-3119(16)61525-3.

Zuil, S. G., Izquierdo, N. G., Luján, J., Cantarero, M., & Aguirrezábal, L. A. N. (2012). Oil quality of maize and soybean genotypes with increased oleic acid percentage as affected by intercepted solar radiation and temperature. *Field Crops Research*. https://doi.org/10.1016/j.fcr.2011.11.019.